Climate Dynamics
https://doi.org/10.1007/s00382-019-04707-2

Mean warming not variability drives marine heatwave trends

Eric C. J. Oliver[1]

Received: 1 May 2018 / Accepted: 1 March 2019

Abstract
Marine heatwaves have been shown to be increasing in frequency, duration and intensity over the past several decades. Are these changes related to rising mean temperatures, changes to temperature variability, or a combination of the two? Here we investigate this question using satellite observations of sea surface temperature (SST) covering 36 years (1982–2017). A statistical climate model is used to simulate SST time series, including realistic variability based on an autoregressive model fit to observations, with specified trends in mean and variance. These simulated SST time series are then used to test whether observed trends in marine heatwave properties can be explained by changes in either mean or variability in SST, or both. We find changes in mean SST to be the dominant driver of the increasing frequency of marine heatwave days over approximately 2/3 of the ocean; while it is the dominant driver of changes in marine heatwave intensity (temperature anomaly) over approximately 1/3 of the ocean. We also find that changes in mean SST explain changes in both MHW properties over a significantly larger proportion of the world's ocean than changes in SST variance. The implication is that given the high confidence of continued mean warming throughout the twenty-first century due to anthropogenic climate change we can expect the historical trends in marine heatwave properties to continue over the coming decades.

Keywords Extreme event · Climate change · Stochastic model · Sea surface temperature

1 Introduction

Marine heatwaves (MHWs) are climatic extremes with real ecological and socioeconomic consequences (Smale et al. 2019). A number of prominent events have ocurred recently including "the Blob" in the North Pacific (Bond et al. 2015; Di Lorenzo and Mantua 2016) and the major coral bleaching event across Northern Australia (Hughes et al. 2017; Benthuysen et al. 2018). MHWs can even cause ecosystem regime shifts, such as from a dominance of kelp forests to that of seagrass meadows after the 2011 event off Western Australia (Wernberg et al. 2013). Therefore the potential for long-term changes in MHWs with climate changes remain a major concern (Frölicher and Laufkötter 2018). In fact, sea surface temperature records indicate significant trends in MHWs over the past several decades, with a > 50% increase in annual MHW days from 1925 to 2016 and a ca. 20% increase in MHW intensity over the satellite period (since 1982; Oliver et al. 2018).

Changes in the frequency and intensity of MHWs may arise to to increases in the mean sea surface temperature (SST) or changes in its variability. A classic representation is shown in Fig. 1 where we see that the area under the upper tail of the probability distribution of temperature (i.e., the likelihood of a marine heatwave, the area shown in pink) can be increased (the union of pink and red areas) either by shifting the distribution (i.e., a rising mean SST, Fig. 1a) and/or widening the distribution (i.e., an increase in SST variability, Fig. 1b). Regional changes to mean SST and SST variability are known to have occurred in the ocean. While globally, mean SSTs are rising (Stocker et al. 2013), regionally there are hotspots of greater increase [e.g., Western Boundary Currents, Wu et al. (2012)] as well as regions barely warming at all or even cooling [e.g., the North Atlantic "warming hole", Drijfhout et al. (2012)]. SST variability changes are also non-uniformly distributed with hotspots such as off southeastern Australia (Oliver et al. 2014) often driven by changes in the mesoscale eddy field (Stammer 1997; Woodworth and Menendez 2015).

Eric C. J. Oliver
eric.oliver@dal.ca

[1] Department of Oceanography, Dalhousie University, Halifax, Nova Scotia, Canada

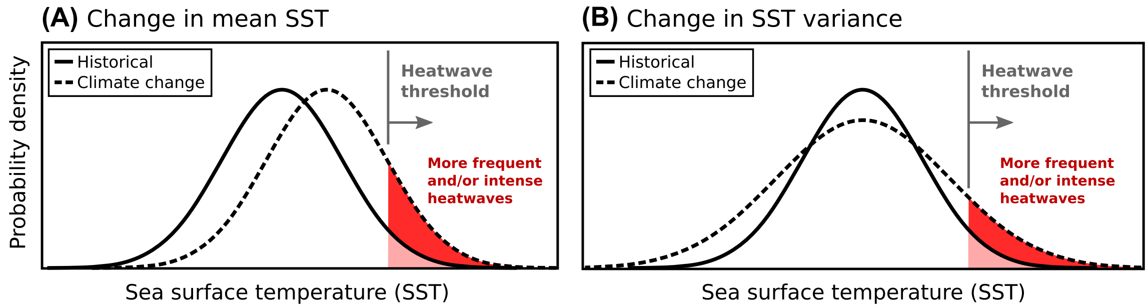

Fig. 1 The effect of changing **a** the mean SST and **b** the variance of SST on the likelihood of extremes (marine heatwaves). Adapted from Field et al. (2012), Fig. SPM.3

While changes to both the mean and variability of SST are conceptually important in driving marine heatwave trends, the relative role of each has not yet been explored in the real ocean. Here we investigate this question, on a global scale, using a simple statistical climate model. The observed ranges of mean warming and trends in variability over the satellite record are used to drive this statistical model, from which are derived the trends in MHW properties. We find that changes in MHW exposure time (total annual MHW days) is dominated by increases to mean SST. On the other hand, for changes in MHW intensity (SST anomaly), neither mean nor variance changes are responsible over most of the global ocean but variance does play an increased importance than it did for MHW exposure.

2 Methods

We used a statistical climate model to simulate trends in MHW properties due solely to trends in the mean or variance of SST. First, we statistically simulated a daily SST time series with stationary statistical properties, meaning its mean and variance do not change with time, using a first-order autoregressive (AR1) model:

$$T(t + \Delta t) = aT(t) + \epsilon(t), \tag{1}$$

where $T(t)$ is SST at time t, Δt is the time step (taken here to be 1 day), a is the autoregressive parameter, and $\epsilon(t)$ is a white noise process [assumed to be normally distributed with mean zero and variance σ_ϵ^2; Priestley (1981)]. This model is based on the concept that a slow system (i.e., the dynamic ocean) can be represented by a red noise signal (T) generated by the integration of stochastic forcing [$\epsilon(t)$, i.e., weather noise; Hasselmann (1976)]. In the present study, this model represents the temperature of a motionless mixed later forced by noisy surface heat fluxes (Frankignoul and Hasselmann 1977). The temperature time series, being red noise, has an inherent memory time scale τ (in days) which can be calculated by a transformation of the autoregressive parameter: $\tau = -1/\ln(a)$.

Given a time series of observed SST, T_o, the AR1 model parameters can be fit as follows. First remove the seasonally varying climatological mean and the linear trend. Then, a is determined by ordinary least squares regression of T_o lagged with itself by 1 day, and σ_ϵ by the standard deviation of the residuals. The model parameters were fit to daily SSTs from the National Oceanic and Atmospheric Administration (NOAA) Optimum Interpolation (OI) SST V2 high resolution (1/4°) gridded SST data over 1982–2017 (Reynolds et al. 2007; Banzon et al. 2016). Large values of the autoregressive time scale τ could be found in the equatorial eastern Pacific (up to 70 days), the eddy-rich western boundary current extensions (30–50 days), and the mid-latitude gyres (10–30 days; Fig. 2a), indicating SST in these regions have longer memories (are more red noise-like). Lower values (< 10 days) were found at very high latitudes and in the Tropics (excluding the eastern Pacific). Large values of the error standard deviation σ_ϵ could be found in the western boundary current regions (including the extensions; up to 0.7 °C), eastern boundary current upwelling systems (0.3–0.5 °C), and much of the equatorial band (0.2–0.5 °C; Fig. 2b). Lower values (< 0.2 °C) were found in the central zones of the mid-latitude gyres. Note that this pattern is generally consistent with the observed pattern of SST variance [e.g., see Fig. 4 in Deser et al. (2010)]. The two-dimensional probability distribution of (τ, σ_ϵ) across all ocean pixels peaks at $\tau = 12$ days and $\sigma_\epsilon = 0.27$ °C; with most values (99%) in the range of $\tau = [5.4, 45]$ days and $\sigma_\epsilon = [0.16, 0.46]$ °C (Fig. 2c).

In order to test for the roles of changing SST mean or variability on the resultant extremes we did the following. Given a set of parameters (τ, σ_ϵ), and random white noise data $\epsilon(t)$, we simulated a stationary daily SST time series covering 36 years (e.g. 1982–2017) using Eq. 1. Since this time series is stationary it has no long-term trend in mean SST or SST variance. We then modified this time series by specifying a constant linear trend in either (i) mean SST

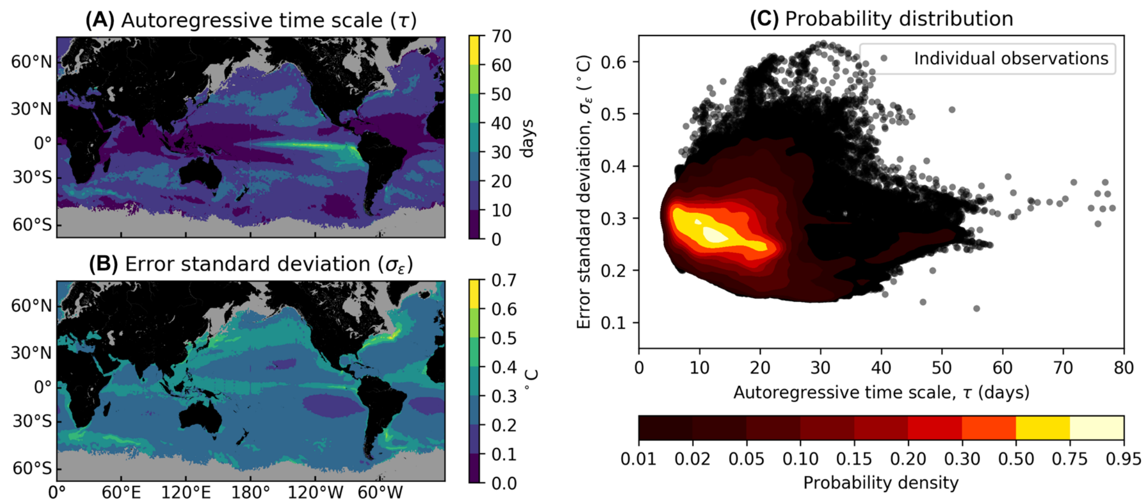

Fig. 2 Parameters for the AR1 stochastic climate model fit to NOAA OI SST over 1982–2017, for each pixel globally. Shown are **a** the autoregressive time scale τ and **b** the standard deviation σ_ϵ of the white noise error forcing. **c** The probability density function of all (τ, σ_ϵ) values

or (ii) SST variance (see "Appendix" for details). MHWs were defined as periods when SSTs were above the seasonally-varying 90th percentile, for at least five consecutive days [see Hobday et al. (2016) for details]. MHW exposure was then defined as the count of MHW days in each year, and MHW intensity as the maximum SST anomaly during any MHW in each year. This was repeated for $N_\epsilon = 500$ independent realisations of $\epsilon(t)$ to generate an ensemble of MHW trends, each representing a different realisation of SST variability. From this ensemble we calculated a 95% confidence interval on the trends in MHW properties, and if this confidence interval does not include zero the trend is considered significant ($p < 0.05$).

In the case of a prescribed trend in mean SST, the statistical properties of the SST time series pertaining to short-term variability remained stable over the entire record (i.e., a constant SST variance), only the mean SST was allowed to vary. Therefore, this confidence interval provided the range of MHW trends that we expect solely from a change in the mean SST itself. In the case of the prescribed trend in SST variance, the mean SST remained the same and so the confidence interval provided the range of MHW trends that we expect solely due to a change in the SST variance. Then, separately for MHW exposure and intensity, we can define four situation types:

- Type 1: trends in the MHW metric due to both SST mean and variance trends are not significantly different from zero (Fig. 3a).
- Type 2: trend in the MHW metric due to SST mean trend is not significantly different from zero, but trend due to SST variance trend is significant (Fig. 3c).

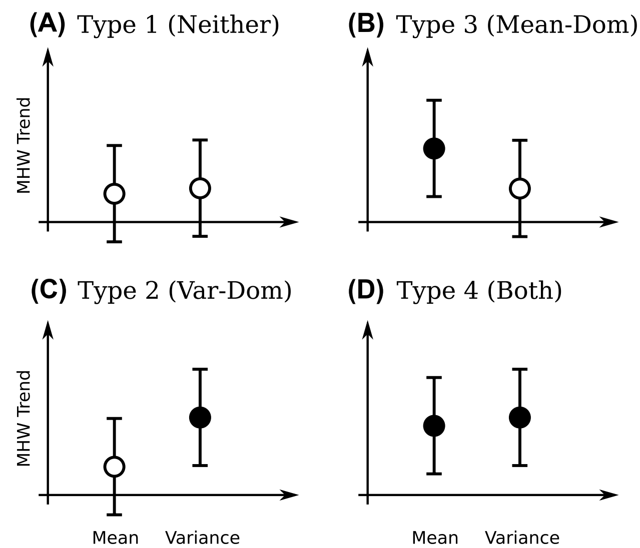

Fig. 3 Description of the four trend types. Each panel indicates a situation type, with the two circles (and error bars) indicating the trend (and confidence interval) in the indicated MHW metric due to trends in the mean (left) or variance (right). Trends that are statistically significantly different from zero are shown as a filled black circle; otherwise an open circle

- Type 3: trend in the MHW metric due to SST variance trend is not significantly different from zero, but trend due to SST mean trend is significant (Fig. 3b).
- Type 4: trends in the MHW metric due to both SST mean and variance trends are significant (Fig. 3d).

We can interpret these types as follows. Type 1 indicates a situation where we do not expect significant MHW trends to be driven by either mean warming or changes in variability (Neither). Type 2 indicates a situation where MHW trends are dominated by trends in SST variablity (Var-Dom), while Type 3 indicates a dominance of mean warming (Mean-Dom). Type 4 indicates that both variability trends and mean warming are important in determining MHW trends (both).

We wish to test the global distribution of the four types in the real ocean, given the observed trends in SST mean and variance and a fit of the AR1 model to the observed SST time series. This could be accomplished by looping over all pixels, globally, and running the Monte Carlo simulation N_ϵ times as described above at each pixel. However, this would require $> 10^5$ independent simulations and would be prohibitively time consuming. Instead, we first pre-calculate the Monte Carlo simulation results for a specified set of (τ, σ_ϵ) values, chosen to uniformly sample the area enclosing 99% of the pdf shown in Fig. 2c. Values were chosen on a regular grid with step of $\Delta\tau = 2$ days and $\Delta\sigma_\epsilon = 0.02\,°\mathrm{C}$. The Monte Carlo trend simulation is then performed for each of these subsampled AR1 parameter values, leading to only 349 independent simulations needed. In addition, for each (τ, σ_ϵ) value the simulations are run for a preselected set of mean SST and SST variance trends. The range of mean and variability trends were determined based on the observed linear trends fitted to the NOAA OI SST data (Fig. 4a, b). The majority of mean warming (variance) trends are between − 0.4 and 1 °C decade^{-1} (− 0.2 and 1.5 °C^2 decade^{-1}; Fig. 4c); the pre-selected set of trends used were [− 0.4, − 0.2, − 0.1, 0, 0.1, 0.2, 0.4, 0.6, 0.8, 1.0]°C decade^{-1} for mean SST and [− 0.2, − 0.1, 0, 0.1, 0.2, 0.35, 0.5, 0.75, 1.0, 1.5]°C^2 decade^{-1} for SST variance. Then, for each pixel the nearest value of subsampled AR1 parameters (τ, σ_ϵ) and trends to the true values (the true values shown in Figs. 2a, b and 4a, b) is chosen and the pre-calculated Monte Carlo simulation results are used to determine which of the four types is present at the pixel.

3 Results

The relationship between trends in MHW metrics and trends in SST mean and variance are demonstrated for a representative SST time series, generated using the most probable model parameter values (the peak in Fig. 2c: $\tau = 12$ days and $\sigma_\epsilon = 0.27$ °C). Both MHW exposure and intensity rise with increasing mean SST (Fig. 5a, c) and with increasing SST variance (Fig. 5b, d). MHW exposure and intensity trends increase nearly linearly with increasing trends in SST mean (Fig. 5a, c), while they increase non-linearly with increasinig trends in SST variance (Fig. 5b, d).

MHW exposure trends are much larger for trends in mean SST (up to ~ 60 days decade^{-1}) than for trends in SST variance (up to 10 days decade^{-1}). Importantly, exposure trends saturate at ~ 10 days decade^{-1} for variance trends larger than > ca. 0.5 °C decade^{-1} (Fig. 5b) while they continue to rise to much greater than 10 days decade^{-1} with increasing mean SST trends (Fig. 5a). Intensity trends on the other hand tend to be of a similar order of magnitude over the representative range of mean and variance trends considered (up to ~ 1 °C^2 decade^{-1}; Fig. 5c, d).

Given an observed trend in SST mean and variance, we can then determine from plots like Fig. 5 if trends in MHW properties are significantly different from zero. This has been performed for the entire ocean, globally, as described in the Methods (Sect. 2). Globally, the Type 3 (Mean-Dom) situation is most common for MHW exposure (Fig. 6a, orange), implying a dominance of mean warming in driving trends in MHW exposure. Nearly

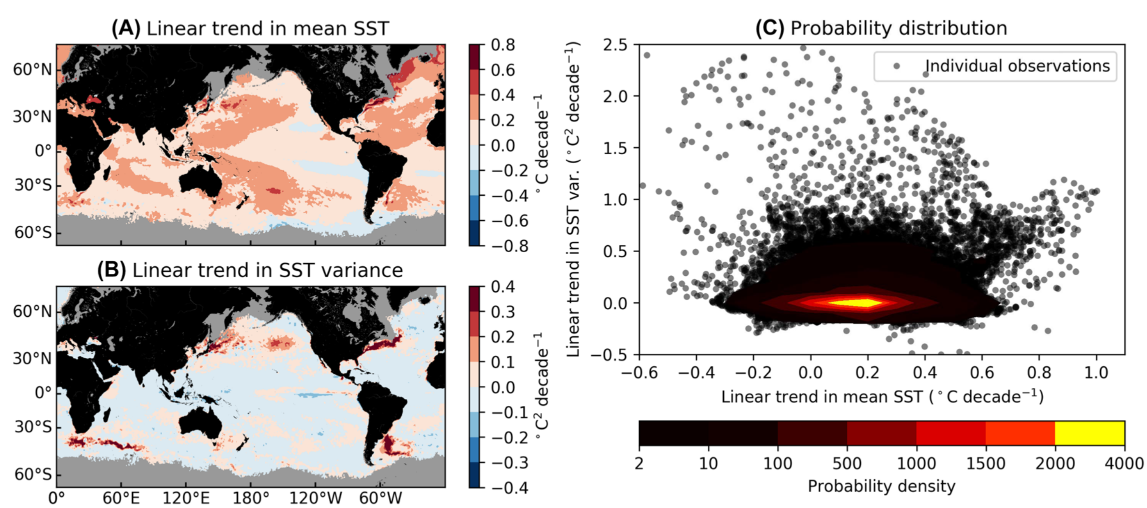

Fig. 4 Shown are linear trends in **a** annual mean SST and **b** annual SST variance from NOAA OI SST over 1982–2017. **c** Probability distribution of all mean and variance trend values shown in **a**, **b**

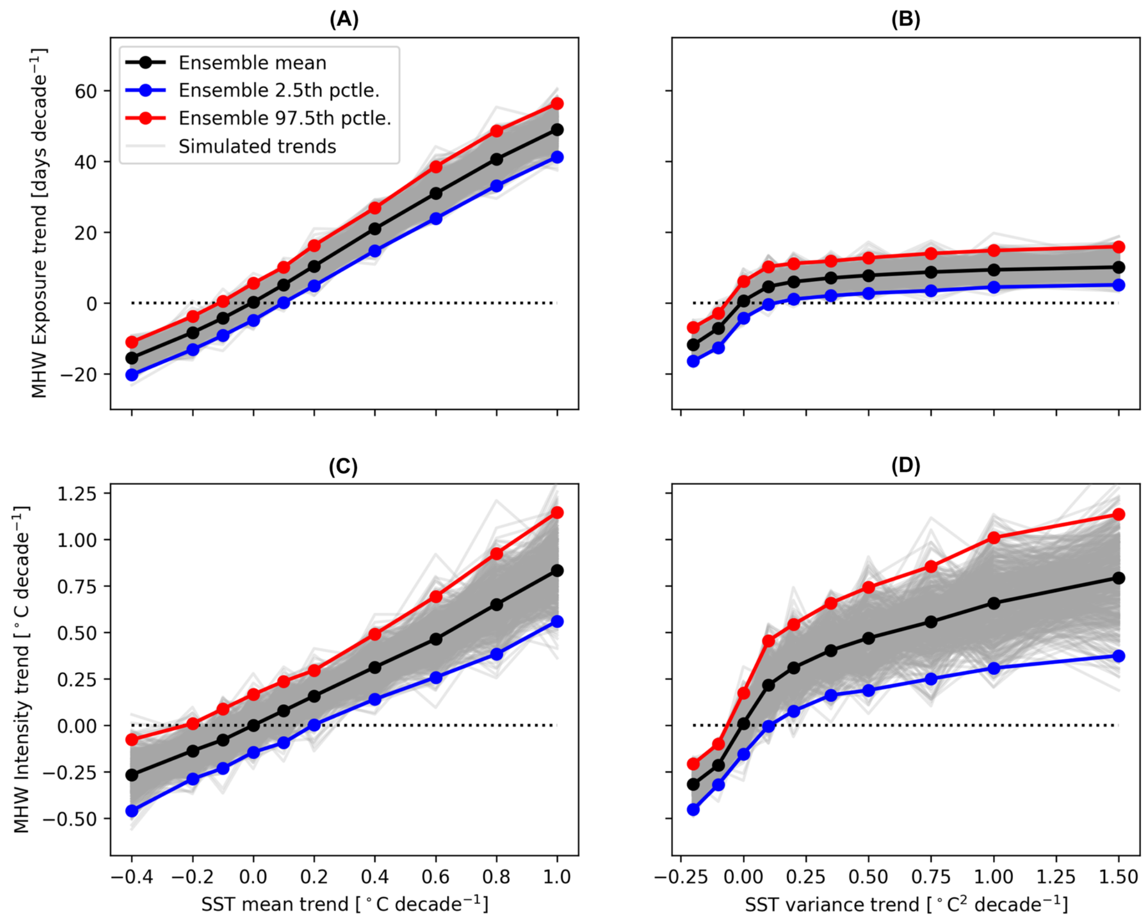

Fig. 5 Simulated MHW trends as a function of trends in mean and variance of SST. Trends in **a**, **b** MHW exposure and **c**, **d** MHW intensity are shown over a range of trends in **a**, **c** mean SST and **b**, **d** SST variance. The grey lines indicate the $N_\epsilon = 500$ ensemble of individual simulations, with model parameters $\tau = 12$ days and $\sigma_\epsilon = 0.27$ °C, while the black, blue and red lines indicate the ensemble mean, 2.5th percentile, and 97.5th percentile, respectively. The interval between the blue and red lines indicates the 95% confidence interval

two-thirds of the ocean surface (63.9%) exhibit Type 3 with most of the remainder indicating Type 1 (32.2%, no significant MHW exposure trends; Fig. 6a, white). Very little of the ocean surface exhibits Type 2 (0.7%; Fig. 6a, blue) or Type 4 (3.2%; Fig. 6a, red) conditions, indicating that trends in variance are only important in driving MHW exposure trends over a total of 3.9% (Types 2 and 4) of the ocean surface.

For MHW intensity trends, the we now see a dominance of Type 1 (60.8%, neither mean or variance dominant; Fig. 6b, white) followed by Type 3 (34%; Fig. 6b, orange). We also see an increased role for SST variance trends, with 5.1% (Types 2 and 4 together; Fig. 6b, blue and red respectively) of the ocean surface having MHW trends driven solely or in part by trends in SST variance. Notably, the role of SST variance is primarily isolated to the mid-latitude western boundary current and extension regions, which are regions of strong SST variance dominated by mesoscale eddies.

4 Discussion

We have addressed the question: are recent changes in marine heatwave properties related to rising mean temperatures, changes to temperature variability or a combination of the two? We investigated this question using global satellite observations of SST (1982–2017) and a statistical climate model which provided simulated SST time series, with prescribed trends in mean and variance. We find that mean SST change was the dominant driver of increasing MHW exposure over nearly two thirds of the ocean, and of changes in MHW intensity over approximately one third of the ocean. We also find that changes in mean SST explains changes in both MHW properties over a significantly larger proportion of the world's ocean than changes in SST variance. Interestingly, for MHW intensity neither mean SST nor SST variance changes are responsible over most of the global ocean but, variance does play an increased importance than it did for MHW exposure. The influence of SST variance changes

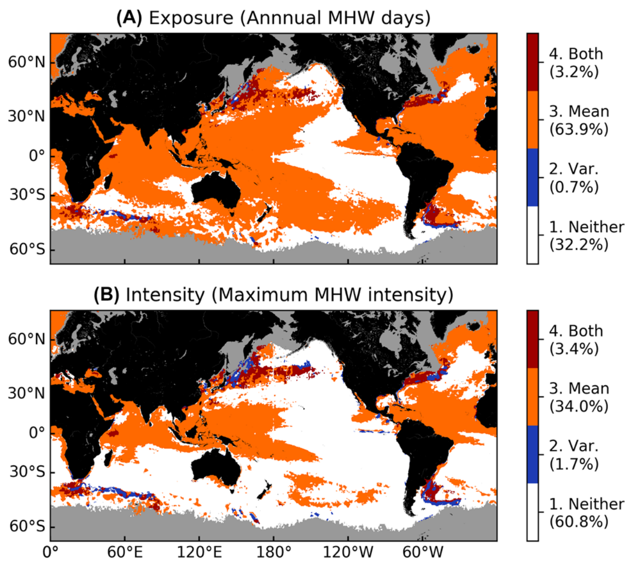

Fig. 6 Relative importance of changes in mean and variance of SST in driving changes to MHW exposure and intensity. The colours indicate whether trends in **a** MHW exposure and **b** MHW intensity are dominated by trends in SST variance and/or mean SST. The four situation types are shown as neither in white, variance-dominated in blue, mean-dominated in orange, and both in red. The proportion of the globe covered by each type is indicated in the colour bar

on MHWs appeared to be primarily restricted to the highly variable mid-latitude western boundary current regions.

It may be noted that we are drawing conclusions about long-term mean warming from a relatively short (in climate terms), multi-decadal dataset. Therefore, we are not testing directly the trends in MHW properties from centennial-scale trends due to climate change. However, the statistical methodology is such that we are elucidating the relationship between short-term SST variations (i.e., MHWs) and changes in the statistical properties of the time series (mean, variance). Therefore, the conclusions drawn from this study should hold regardless of the sources of change in those statistical properties (e.g., climate change, or multi-decadal variability).

Our findings imply that continued rising mean ocean temperatures, which is projected to occur under current greenhouse gas emission levels, will have a strong effect on continued increases in MHW exposure globally. This warming will have somehwat lesser but still important effect on MHW intensity. However, given that neither mean nor variance of SST was found to be the dominant driver of MHW intensity changes over most of the ocean it is less clear what is driving trends in that metric. Therefore, the future state of MHW intensity is less easy to project based solely on mean SST trends.

Acknowledgements This study makes a contribution to the International Marine Heatwaves Working Group (http://www.marineheatwaves.org). NOAA High Resolution SST data provided by the NOAA/OAR/ESRL PSD, Boulder, Colorado, USA, from their Web site at https://www.esrl.noaa.gov/psd/. This work was supported by the National Sciences and Engineering Council of Canada (NSERC) Discovery Grant RGPIN-2018-05255.

Appendix

Start with a stationary time series $T(t)$, where t is time, with mean $\mu = 0$ and variance σ^2. The mean and variance do not change with time. We wish to generate two new time series: $T_m(t)$ which has a linearly increasing mean value (but constant variance σ^2) and $T_v(t)$ which has linearly increasing variance (but constant mean μ).

Increasing mean

Let us define $T_m = T + mt$, where m is a constant. This time series has a mean and variance given by

$$\mu_m = E[T_m] = E[T + mt] = E[T] + mt = \mu + mt = mt, \tag{2}$$

$$\sigma_m^2 = E[(T_m - \mu_m)^2)] = E[(T + mt - \mu - mt)^2] = E[T^2] = \sigma^2, \tag{3}$$

where $E(\cdot)$ is the expectation operator and noting that $E(T) = \mu = 0$. Therefore T_m has a linearly increasing mean and the same (constant) variance as T, σ^2.

Increasing variance

Let us define $T_v = T(1 + vt)$, where v is a constant. This time series has a mean and variance given by

$$\mu_v = E[T_v] = E[T(1 + vt)] = E[T + vtT] = E[T] + vtE[T], \tag{4}$$

$$= \mu + vt\mu = 0, \tag{5}$$

$$\sigma_v^2 = E[(T_v - \mu_v)^2] = E[(T + vtT)^2] = E[T^2 + 2vtT^2 + (vtT)^2], \tag{6}$$

$$= E[T^2] + 2vtE[T^2] + (vt)^2E[T^2] = \sigma^2 + 2vt\sigma^2 + (vt)^2\sigma^2, \tag{7}$$

$$= \sigma^2(1 + 2vt + (vt)^2) \tag{8}$$

and noting that $E(T^2) = \sigma^2$. If we neglect nonlinearities, we can simplify this to a linear dependence on time

$$\sigma_v^2 \simeq \sigma^2 + v^* t, \tag{9}$$

where $v^* = 2v\sigma^2$.

References

Banzon V, Smith TM, Chin TM, Liu C, Hankins W (2016) A long-term record of blended satellite and in situ sea-surface temperature for climate monitoring, modeling and environmental studies. Earth Syst Sci Data 8(1):165

Benthuysen JA, Oliver EC, Feng M, Marshall AG (2018) Extreme marine warming across tropical australia during austral summer 2015–2016. J Geophys Res Oceans 123:1301–1326

Bond NA, Cronin MF, Freeland H, Mantua N (2015) Causes and impacts of the 2014 warm anomaly in the NE Pacific. Geophys Res Lett 42(9):3414–3420

Deser C, Alexander MA, Xie SP, Phillips AS (2010) Sea surface temperature variability: patterns and mechanisms. Annu Rev Mar Sci 2:115–143

Di Lorenzo E, Mantua N (2016) Multi-year persistence of the 2014/15 North Pacific marine heatwave. Nat Clim Change 6(11):1042–1047

Drijfhout S, Van Oldenborgh GJ, Cimatoribus A (2012) Is a decline of AMOC causing the warming hole above the North Atlantic in observed and modeled warming patterns? J Clim 25(24):8373–8379

Field CB, Barros V, Stocker TF, Qin D, Dokken DJ, Ebi KL, Mastrandrea MD, Mach KJ, Plattner GK, Allen SK (2012) Managing the risks of extreme events and disasters to advance climate change adaptation. Cambridge University Press, Cambridge

Frankignoul C, Hasselmann K (1977) Stochastic climate models, Part II application to sea-surface temperature anomalies and thermocline variability. Tellus 29(4):289–305

Frölicher TL, Laufkötter C (2018) Emerging risks from marine heat waves. Nat Commun 9(1):650

Hasselmann K (1976) Stochastic climate models part I. Theory Tellus 28(6):473–485

Hobday AJ, Alexander LV, Perkins SE, Smale DA, Straub SC, Oliver EC, Benthuysen JA, Burrows MT, Donat MG, Feng M (2016) A hierarchical approach to defining marine heatwaves. Prog Oceanogr 141:227–238

Hughes TP, Kerry JT, Álvarez-Noriega M, Álvarez-Romero JG, Anderson KD, Baird AH, Babcock RC, Beger M, Bellwood DR, Berkelmans R (2017) Global warming and recurrent mass bleaching of corals. Nature 543(7645):373

Oliver ECJ, Wotherspoon SJ, Holbrook NJ (2014) Projected Tasman Sea extremes in sea surface temperature through the 21st Century. J Clim 27(5):1980–1998

Oliver ECJ, Donat MD, Burrows MT, Moore PJ, Smale DA, Alexander LV, Benthuysen JA, Feng M, Sen Gupta A, Hobday A, Holbrook NJ, Perkins-Kirkpatrick SE, Scannell HA, Straub SC, Wernberg T (2018) Longer and more frequency marine heatwaves over the past century. Nat Commun 9:1324

Priestley MB (1981) Spectral analysis and time series. Academic Press, New York

Reynolds RW, Smith TM, Liu C, Chelton DB, Casey KS, Schlax MG (2007) Daily high-resolution-blended analyses for sea surface temperature. J Clim 20(22):5473–5496

Smale D, Wernberg T, Oliver ECJ, Thomsen M, Harvey B, Straub S, Burrows M, Alexander L, Benthuysen J, Donat M, Feng M, Hobday A, Holbrook N, Perkins-Kirkpatrick S, Scannell H, Sen Gupta A, Payne B, Moore P (2019) Marine heatwaves threaten global biodiversity and the provision of ecosystem services. Nat Clim Change. https://doi.org/10.1038/s41558-019-0412-1

Stammer D (1997) Global characteristics of ocean variability estimated from regional TOPEX/POSEIDON altimeter measurements. J Phys Oceanogr 27(8):1743–1769

Stocker T, Dahe Q, Plattner GKE (2013) Working group I contribution to the IPCC fifth assessment report climate change 2013, the physical science basis. IPCC

Wernberg T, Smale DA, Tuya F, Thomsen MS, Langlois TJ, De Bettignies T, Bennett S, Rousseaux CS (2013) An extreme climatic event alters marine ecosystem structure in a global biodiversity hotspot. Nat Clim Change 3(1):78

Woodworth PL, Menendez M (2015) Changes in the mesoscale variability and in extreme sea levels over two decades as observed by satellite altimetry. J Geophys Res Oceans 120(1):64–77

Wu L, Cai W, Zhang L, Nakamura H, Timmermann A, Joyce T, McPhaden MJ, Alexander M, Qiu B, Visbeck M (2012) Enhanced warming over the global subtropical western boundary currents. Nat Clim Change 2(3):161–166